REPORT DOCUMENTATION PAGE

AFRL-SR-AR-TR-03-

0492

1. REPORT DATE (DD-MM-YYYY)	2. REPORT TYPE	
06-12-2003	Final Technical Report	Feb 2001-Nov 2003

4. TITLE AND SUBTITLE Dynamic RCS:, A Geometrical/Eulerian Approach to Computing High Frequency Radar Cross Sections

5a. CONTRACT NUMBER

5b. GRANT NUMBER
F49620-01-1-0189

5c. PROGRAM ELEMENT NUMBER

6. AUTHOR(S)
Osher, Stanley and Steinhoff, John

5d. PROJECT NUMBER

5e. TASK NUMBER

5f. WORK UNIT NUMBER

7. PERFORMING ORGANIZATION NAME(S) AND ADDRESS(ES)

Level Set Systems
1058 Embury Street
Pacific Palisades, CA
90272-2501

8. PERFORMING ORGANIZATION REPORT NUMBER
LSS-03F

9. SPONSORING / MONITORING AGENCY NAME(S) AND ADDRESS(ES)
USAF, ARL
AF Office of Scientific Research
801 N Randolph St Room 732
Arlington, VA 22203-1977

10. SPONSOR/MONITOR'S ACRONYM(S)
AFOSR

11. SPONSOR/MONITOR'S REPORT NUMBER(S)

12. DISTRIBUTION / AVAILABILITY STATEMENT
Unlimited distribution, publicly available

20040105 031

13. SUPPLEMENTARY NOTES

14. ABSTRACT
Level Set Systems (LSS) has developed a 3D Eulerian, time domain method for computing the propagation and scattering of short electromagnetic pulses over arbitrarily long distances. Efforts accommodated include variation of index of refraction and scattering from complex features including tanks and aircraft. LSS developed a level set method for the construction of wavefronts that handles resolution, multivalued solutions, reflection and refraction. The key idea involves an Eulerian, fixed grid solver involving a system of linear Liouville equations, three equations in five space dimensions. The complexity of each update is no worse than that of ray tracing because of the use of a new local level set method for high dimension and codimension. This allows this level set method to be a viable alternative to ray tracing with many advantages for realistic DOD applications involving geometric optics. Flow Analysis Inc (FAI) has developed a lattice confinement method that has been shown To be effective for propagating short pulses as nonlinear solitary waves over long distances. These two methods complement each other and lay the foundation for greatly improved Radar Cross Section computations.

15. SUBJECT TERMS
Eulerian, time domain, level set, lattice confinement, Liouville equation, ray tracing

16. SECURITY CLASSIFICATION OF: Unlimited distribution, unclassified UU			17. LIMITATION OF ABSTRACT	18. NUMBER OF PAGES	19a. NAME OF RESPONSIBLE PERSON
a. REPORT	b. ABSTRACT	c. THIS PAGE			Stanley Osher
UU	UU	UU	UU	27	19b. TELEPHONE NUMBER (Include area code) 310-573-9339

Report for AFOSR Grant # F49620-01-1-0189

Stanley Osher
Level Set Systems, Inc
1058 Embury Street
Pacific Palisades, CA 90272-2501
Email: ilevels310@earthlink.net
Phone/fax 310-573-9339

1. INTRODUCTION

Geometric optics makes its impact, both in mathematics and in real world applications related to ray tracing, migration and tomography. The primary objective of this phase of the research has been to develop a 3-D Eulerian time domain method for accurately computing the propagation and scattering of short electromagnetic and acoustic waves over very long distances ($>>10^4\lambda$) through the atmosphere, where λ is the width of the pulse. Effects accommodated include variation of index of refraction and scattering from complex features, such as tanks and aircraft. Of special interest in these problems are the wavefronts, or points of constant travel time away from sources, in the medium. Previously in [OCKST] under the support of this contract, we initiated a level set approach for the construction of wavefronts in isotropic media that handled the two major algorithmic issues of resolution and multivalued solutions. This approach was quite general and we were able to construct wavefronts in the presence of refraction, reflection, higher dimensions and, in other new work supported by this contract [QCO, COQ], we included anisotropy.

However, the technique proposed for handling reflections of waves off objects, the basic phenomenon involved in all applications of geometric optics, was inefficient and unwieldy to the point of being unusable, especially in the presence of multiple reflections. In [CKOST] (enclosed) supported by this contract we introduced an approach based on the foundation presented in [OCKST] that fixes this issue. This reworking fully allows this level set method to be a viable alternative to ray tracing, with many advantages, for realistic applications involving geometric optics, especially applications of interest to DOD.

The main difficulty encountered by all numerical approaches in the construction of wavefronts in the geometric optics or ray tracing setting lies in a choice of either resolution or generation of multivalued solutions. Multivaluedness in wavefronts occur when wavefronts cross and more than one ray occupies a region in space. The formation of the well known phenomenon of caustics originates from this. Solutions obtained following the Lagrangian representation of ray tracing, which involves using the method of characteristics to track the position and ray direction of points on the wavefronts, can automatically produce multivalued wavefronts but have difficulties in resolving wavefronts in general, especially when they are diverging. On the other hand, Eulerian approaches applied to the eikonal equation automatically resolve all wavefronts over an underlying grid in space but encounter difficulties in generating multivalued wavefronts.

We overcame these difficulties in our first paper [OCKST], and now have extended this to anisotropy and reflection. In [JO], we extended the idea to the computation of multivalued solutions to quasi-linear hyperbolic partial equations and Hamilton-Jacobi equations in arbitrary space dimensions. We use the classic idea of Courant and Hilbert to define the solution of the quasi-linear hyperbolic PDEs or the gradient of the solution to the Hamilton-Jacobi equations as zero level sets of level set functions. Then the evolution equations for the level set functions satisfy linear Liouville equations defined in the "phase" space, unfolding the singularities and preventing the numerical capturing of viscosity solution. This provides a computational framework for the computations of multivalued geometric solutions to general quasilinear PDEs. In [CLO], we apply our idea to compute the linear Schrödinger equations with efficiently highly oscillating initial data. The high-frequency asymptotics of these equations lead to the well known WKB system, where the phase evolves according to a nonlinear Hamilton-Jacobi equation and the intensity of the plane wave is governed by a linear conservation law. This becomes equivalent to solving a linear Liouville equation with multi-valued phase as we already developed in [OCKST].

In higher dimensions, computational speed, visualization and efficiency start to become major issues. We have begun successfully attacking these issues and have a local method, involving local memory and an innovative new visualization technique for submanifolds of high dimensional space developed by C. Min and S. Osher[M, MO]. Also, we are investigating a suggestion put forward by F. Reitich and J. Qian that spectral methods be used to update our evolution in the angle variables and discontinuous Galerkin methods be used to update the space variables. Qian and Reitich are using our basic technique and we expect to work with them.

Another advantage of our Eulerian grid based techniques is that it can be updated simultaneously with full Maxwell's equation solvers. We intend to work with our colleagues at Hypercomp, Inc. and Brown University on this. Finally, we are exploring a promising new confinement technique, put forward by our subcontractor, Flow Analysis Inc to help enhance both of these methods.

The Flow Analysis, Inc.'s pulse propagation algorithm involves a new – "Lattice Confinement" Method (LCM) that has been shown to be effective for propagating short pulses (~ 2 cells wide) as non linear solitary waves over arbitrary distances with no numerical spreading. This pulse algorithm, by itself, will be an important contribution to time domain radar scattering techniques.

The short pulses resulting from the LCM have been previously shown to also allow the computation of high frequency time domain phases and amplitudes, including multiple arrival times. This aspect represents an important capability. In this mode, effectively, as the short pulse surface sweeps through the computational grid, new amplitude/phase values will be generated within the band extending across the width of the pulse. After passage of the pulse, these values will be stored in an array so that new pulses, and hence new arriving waves can be treated. This capability has previously been presented in [SWUP].

1.1 Relation to Other Methods

a) Direct Wave Equation Solvers

The LCM will be useful by itself, but will also be able to be matched to other, existing methods/codes, such as direct Maxwell equation solvers [S], which are in use for computing the fields near an object. In this mode, the LCM will serve to extend the solvers far beyond their limit. Since direct solvers resolve the individual waves (even optimized methods [CSE] still must satisfy the Nyquist criterion), the computational requirements limit them to regions of $O(10^2\lambda)$. Thus these methods, alone, are not sufficient to treat long distance propagation, either in the frequency or time domain. This matching feature should be important for low observable objects where complex, well-developed computational methods are already in use near the objects.

(b) Eikonal Schemes

As described above, the LCM will be able to automatically transition to conventional Eulerian solves near a scatterer, if necessary. This appears to be difficult with conventional high frequency Eikonal methods. Also, as described in [SWUP], multiple-arrival times will automatically be accommodated, something difficult for Eikonal schemes [FEO], but which is easy for the vector level set method of LSS.

In this way, the LCM complements the other research discussed in this report.

(c) Kirchhoff Methods

Variable index of refraction effects will be treated, which are not included in conventional Kirchhoff integral methods.

(d) Lippmann Schwinger Integral Schemes

Almost all of the problems to be treated involve waves that pass through each point either once, or only a few times. This includes multiple scattering from surfaces and refraction/ducting effects. In many of these, the physical space can be divided into separate regions that can be computed sequentially – such as the region near a scatter and the far field. This feature can be used by the LCM to easily decompose the computational domain into separate domains to be treated sequentially, thereby greatly reducing memory requirements and allowing parallel computation. This does not appear to be feasible with straightforward implementations of the Lippmann Schwinger integral equation approaches [BK], where each region of space is connected to other regions by a Green's function (assuming varying index of refraction). Further, with the LCM, computations are done only in a narrow band of the grid ($n \sim O(1)$ cells) at each of a number of time steps (N_T). This number is of the order of the grid size in each direction

(say N_X). Thus, for 3-D computations, the total number of computations is only $O(N_X^3)$. Also, each of these computations is a simple, local finite difference operation.

(e) General Frequency Domain Methods

The LCM can be used to compute time domain solutions for long-range propagation/scattering of short pulses, which can be important for modern radar. This appears to be outside the scope of narrow band frequency domain schemes, since short pulses consist of a large frequency band which would require many frequency domain solutions using conventional methods.

(f) Ray Tracing Methods

Ray tracing schemes have well-known difficulties in reconstructing continuous pulse or phase surfaces in general. Also, information must be interpolated onto a uniform grid to be useful for many purposes.

The LCM, as are methods (a) – (e) above, is completely Eulerian. A convenient structured computational grid is used which does not have any special data handling requirements. This grid is suitable for representing variations of the index of refraction, topographic boundary conditions and the geometries of scattering objects. Also, transmission and scattering amplitudes and phases, if they are to be useful, should be represented on a convenient, structured grid.

The following Level Set Systems, Inc. personnel were supported under this grant: Dr. Stanley Osher, Dr. Susan Chen, Dr. Hyeseon Shim and Dr. Myungjoo Kang. The following Flow Analysis, Inc. personnel were supported under this grant: Dr. John Steinhoff and Dr. William Dietz.

2. LEVEL SET FORMULATION AND VISUALIZATION

For purpose of simplicity and exposition, we restrict to our attention to n = 2 for formulation, but we will give the result for higher dimension too. Thus reduced phase space, for a fixed time, can be written as the set of (x,θ), where $x \in R^2$ and $\theta \in [-\pi,\pi]$, θ being the angle of p in polar coordinates. So for a fixed time, the representation of the wavefront, called bicharacteristic strip, is a smooth curve in reduced phase space. In our formulation, the curve is represented by the intersection of two surfaces, which in turn are represented by the zero level sets of two level set functions. Denoting the level set functions by ϕ and ψ, the curve is thus the set of points where $\phi = \psi = 0$. The Liouville equation on each level set function, written as

$$\begin{aligned} \phi_t + v \cdot \nabla_{x,\theta} \phi = 0 \\ \psi_t + v \cdot \nabla_{x,\theta} \psi = 0 \end{aligned} \qquad (2.1)$$

where θ denotes the phase plane angle and v is given by

$$v(x,\theta)=\begin{pmatrix} c(x)\cos\theta \\ c(x)\sin\theta \\ c_{x_1}(x)\sin\theta - c_{x_2}(x)\cos\theta \end{pmatrix} \qquad (2.2)$$

where c is the given local wave velocity permitted in the medium. Also note these two transport equations in ϕ and ψ can be solved separately. For the case of refraction, we use the smooth delta function between two medium to avoid the sudden jump which may create the instability in numerical calculation. For the case of reflection, we consider it as an initial boundary value problem, i.e., we give the boundary condition on the reflected wall whenever it needed and solve the Liouville equation with those boundary conditions. In 3 dimensional cases, we can still use a uniform grid without any problem. But for higher dimensional cases (n > 2), it is almost impossible to use a uniform mesh to simulate our optics problems. The reason is that we need humongous memory and time to get a piece of result in higher dimension. One more issue in higher dimension cases is how to visualize our results. For n = 3 (i.e., we need 5 dimensional calculation), our result surface is the intersection of three 4 dimensional zero level isosurfaces.
In order to overcome those issues, we used a new local level set method and visualization technique developed by C. Min and S. Osher [M, MO]. We can reduce the numerical cost for both memory and time as much as $O(n^2)$ ratio for n = 3.

3. The Lattice Confinement Method

3.1 Basic Features

The main requirement of the method is to compute thin propagating wave equation pulses that do not spread due to numerical effects.

The LCM efficiently simulates these wave equation pulses, in Eulerian computations on fixed, coarse grids. The method involves treating the features as solitary waves that obey nonlinear, difference equations, which are different from Taylor expansion– based discrete approximations to the governing, partial differential equations (pde's). These equations are rotationally invariant generalizations to multiple dimensions of 1-D discontinuity confinement schemes. The method is a generalization of an earlier method, "Vorticity Confinement" [SU], which was successful in efficiently treating thin, vortical regions.

For long distance propagation of pulses, direct discretization and solution of the governing partial differential equations (pde's) using conventional Eulerian Taylor expansion–based numerical methods to resolve the thin features can be prohibitively expensive. Even adaptive unstructured grid methods are very expensive and complex for general problems with many small-scale, time-dependent features. Fortunately, the details of the internal structure of these small features are often not as important as integral quantities. The quantities of importance for our purpose are the centroid motion and total integrated amplitude at each point along the pulse surface. The main issue in computing these cases is that conventional pde-based methods require a relatively large number of grid cells (4-8) across each small dimension to treat a feature, such as a wave equation

pulse. Even then, the details of the internal structure will be mainly determined by the discrete numerics, and not the physics of the pde. Also, numerical discretization errors will still build up over long distances, causing, for example, large, unphysical spreading.

This leads us to the idea of simulating or "modeling " the thin features directly on the grid with *difference* equations, rather than attempting to accurately discretize the pde's for them using *finite difference* approximations. The idea of modeling, or solving for small-scale features directly on the grid without using smoothness assumptions or Taylor expansions, i.e., as "weak solutions", goes back to work of Lax and others [L], but was applied mostly to shocks. Shocks, however, effectively, "capture themselves" because they have converging characteristics. Harten [H] did treat contact discontinuities in this way, which do not have converging characteristics, but for 1-D compressible flow.

A major difference between the LCM and conventional discontinuity steepening schemes is that LCM is not a concatenation of 1-D operators along each axis, but is intrinsically rotationally invariant.

First, the Lattice Confinement Method will be reviewed for wave equation pulses. Some results will then be presented for short scalar pulses. Previous results [SDHXLF] for a 2-D pulse reflecting from planar surfaces will be shown, then 3-D results for a pulse reflecting from complex objects (a missile and an aircraft). The missile case will involve multiple, curvilinear grids.

3.2 Basic LCM Algorithm

(Parts of this section are related to Ref. [SDHXLF])

As mentioned, the main idea is to treat thin features as nonlinear solitary waves that "live" directly on the grid lattice, spread over only a few cells. The internal structure is determined by the discrete lattice equations. The total amplitude, centroid and (in a future extension), a few moments, however, are determined by the physics. These quantities are transported across the grid with essentially no numerical errors.

Essentially, these discrete equations define a simple, implicit model which obeys a "fast" dynamics, relaxing to an asymptotic, propagating state in a few time steps. In this way we can simulate the most important physical effects of the small scales, which cannot be accurately computed by just discretizing the governing pde's on the given grid. These effects can be, for example, that thin wave equation pulses propagate over long distances without spreading in a smooth, slowly varying external field, and that they can merge or reflect, respectively, and thus change topology.

3.2.1 Stationary Case

The formulation presented here is related to that presented in [FWS] in 1-D. First a stationary pulse is discussed, requiring only an iteration of the Lattice Confinement terms, so that the simple asymptotic form can be seen. Advection, in general, will change this form somewhat. However, in the limit of small advection time step, or if a number of

these "Confinement" steps are taken for each convection step, then the following form should result. The same is true for the wave equations. Results very close to these are also found with advection steps that are not small; these are shown in Ref. [FWS].

We start with an iteration for a single-signed scalar, ϕ:

$$\partial_t \phi = \frac{h^2}{\Delta t} \nabla^2 [\mu\phi - \varepsilon\Phi]$$

or

$$\phi^{n+1} = \phi^n + h^2 \nabla^2 (\mu\phi^n - \varepsilon\Phi^n) \qquad (3.1)$$

where Φ is a nonlinear function of ϕ (given below) and μ is a diffusion coefficient that can include numerical effects in a convection or wave equation solution (we assume physical diffusion is much smaller). The discretized grid cell size is h and time step, Δt. For the last term, ε is a numerical coefficient that, together with μ, controls the size and time scales of the confined features. For this reason, we refer to the two terms in the brackets as "Confinement terms".

The two (positive) parameters, ε and μ, are determined by the two small scales of the computation, h and Δt, since we want the small features to relax to their solitary wave shape in a small number of time steps and to have a support of a small number of grid cells. Thus, even though h may be small, the Laplacian will be large and the total effect also large.

For the propagating pulse problem, it is assumed that the slowness field is slowly varying compared to these scales. Relaxation of this assumption to accommodate discontinuity is straightforward. We then have a two-scale problem with the thin structure obeying a "fast" dynamics:

$$\mu\phi - \varepsilon\Phi \approx 0 .$$

With propagation in a "slow", smooth external field, this relation is still approximately satisfied, as verified by computations and heuristic arguments [SDHXLF].

There are many possibilities for Φ. A simple class is

$$\Phi^n = \left[\frac{\sum_l C_l (\tilde{\phi}^n)^{-\rho}}{\sum_l C_l} \right]^{-1/\rho} \qquad (3.2)$$

$$\tilde{\phi}^n = |\phi|^n + \delta .$$

The above sum is over a set of grid nodes near and including the node where Φ is computed. The absolute value is taken and δ, a small positive constant ($\sim 10^{-8}$), is added to prevent problems due to finite precision. The coefficients, C_l, can depend on l, but

good results for many cases are obtained by simply setting them as well as ρ to 1. Then, Φ is the harmonic mean of ϕ on the local stencil. Other forms could also be used, with $\rho>1$. $\rho=\infty$ corresponds to the minimum of the absolute value: for 2-D and 3-D applications discontinuous operators such as "min" will not result in as smooth distributions as continuous ones, and we use only $\rho=1$ or $\rho=2$.

An important feature of Lattice Confinement is that all terms are homogeneous of degree 1 in Eqn. 3.1 (as they are in the original wave equation). This is necessary because the Lattice Confinement terms should not depend on the scale of the quantity being confined. Another important point is that wavelengths longer than the thin features that are to be confined must have a negative diffusive behavior, so that the features remain confined, that is stable to perturbations against spreading. This means that Φ must be nonlinear: It is easy to show by Von Neumann analysis that a linear combination of terms, for example of second and fourth order, cannot lead to a stable Confinement for any finite range of coefficients: any wavelength that exhibits negative diffusion would then eventually diverge.

3.3 Wave Equation Formulation

We start with the 1-D scalar wave equation with constant wave speed, c, for simplicity. As in scalar convection, we add an additional term to control the shape of a short pulse:

$$\partial_t^2\phi = c^2\partial_x^2\phi + \partial_x^2\psi$$

or, using a simple time discretization,

$$\phi^{n+1} - 2\phi^n + \phi^{n-1} = c^2\Delta t\partial_x^2\phi + \Delta t\partial_x^2\psi \qquad (3.3)$$

It was seen in [SDHXLF] that the addition of "Lattice Confinement" terms in the form of second derivatives of a function that decays sufficiently rapidly away from the centroid do not change the propagating speed (nor the total amplitude) of a propagating, confined pulse. The same is true here. This means, of course, that they do not change the motion of the centroid of an isolated pulse.

The main constraint on the Confinement term ψ, is that it force an initial isolated, propagating compact pulse with a single maximum to remain compact and not develop any additional maxima. We use:

$$\psi^n = \mu\delta_n^-\phi^n - \varepsilon\delta_n^-\Phi^n\left(\phi^n\right) \qquad (3.4)$$

In this term Φ has the form given by Eqn. (3.2) in terms of its argument. We have defined

$$\delta_n^- f^n = f^n - f^{n-1}$$

Results will be given in Sec. 4 using this form.

An important feature of the method is that the wave do not suffer a "phase shift" when they pass through each other. This is obvious for the equation we want to simulate – the linear wave equation. However, the Confinement term is nonlinear. Such a phase shift would show up as a kink in two waves in 2 or 3 dimensions that are passing through each other, and can be studied in detail in 1-D. It turns out that there is no kink, to plottable accuracy, as can be seen in the plotted scattering results in Sec. 4. Results for the centroid trajectories for 2 pulse passing through each other in 1-D are presented in Fig. 8. There, the computed centroids are plotted as solid lines and the exact as dashed (the periodic boundary conditions can be seen in the former). It can be seen that there is no phase shift to plottable accuracy. This lack of nonlinear interaction persists, according to our study, in the limit of small time step (2 orders of magnitude smaller that that of Fig. 8), even though $O(10^2)$ confinement corrections were applied as the pulses were overlapping. We attribute this to the existence of another conserved variable, similar to total energy. This computation was done by Nick Lynn of University of Tennessee Space Institute (UTSI) under separate funding.

Another important study involves the pulse speed in non-uniform slowness fields. This problem was suggested by Alan Newell. For an initially circular pulse in 2-D propagating through regions where slowness varied by a factor of 5 across the circle, numerical errors in the speed were insignificant to plottable accuracy. This was verified by varying the grid size by a factor of 40 in each direction. (This was done by Meng Fan of UTSI under separate funding.)

One other important use of Lattice Confinement for the wave equation involves cases with multiple grids with grid interfaces. These are used in the missile reflection problem described in Sec. 4. If only the discretized wave equation is used, with no Confinement, reflections result from small numerical errors at the grid interfaces, unless special care is taken. Lattice Confinement completely overcomes this problem and the (single) pulse propagates across the interface with no reflections.

Some of the advantages of using direct difference equations instead of pde's for a related problem can be found in [CSE]. There, a very efficient formulation is derived for the Helmholtz equation by minimizing the L_2 norm of the error of waves propagating with fixed $|\vec{k}|$.

3.4 Vector Potential Formulation

In a recent promising development in our wave equation research, we have implemented a vector potential, $\vec{A}$, as the basic variable, instead of a scalar representing the magnitude of the $\vec{B}$ field. Even though there is no direct effect of this change in classical electromagnetics, there is a major advantage in the computation of pulse solutions. This is because, for a thin pulse, $\vec{E}$ and $\vec{B}$ only have a small region of support, but $\vec{A}$ extends throughout the field. The $\vec{E}$ and $\vec{B}$ representation of the pulse is a spread

delta function across the width, but the $\vec{A}$ representation is a step function. As a result, it is much easier to capture the pulse by operating on $\vec{A}$, since it is topologically "trapped" by this field. The argument is exactly the same as in Vorticity Confinement, where thin vortical regions ($\vec{\omega}$) are trapped in a velocity field, $\vec{q}$, which extends throughout space. (This is also related to the trapping of defects in other field theories). The resulting confinement terms are exactly the same in the two cases, with $\vec{A}$ corresponding to $\vec{q}$ and $\vec{B}$ corresponding to $\vec{\omega}$.

The formulation is

$$\vec{B} = \vec{\nabla} \times \vec{A} \qquad (3.5)$$
$$\delta_t^2 \vec{A} = c^2 \nabla_D^2 \vec{A} + \mu \delta_t \nabla_D^2 \vec{A} + \varepsilon \delta_t \vec{\nabla}_D \times \vec{b}$$

where $\vec{b}$ is a local harmonic mean of $\vec{B}$ at each grid point:

$$\vec{b} = \frac{\vec{B}}{|\vec{B}|}\left[\sum_{\ell} \frac{|\vec{B}_\ell|^{-1}}{N}\right]^{-1}$$

and where δ_t and ∇_D denote discrete operators and Eqn. 3.5 was used with a sum over N neighboring points, labeled ℓ. In the formulation the Coulomb gauge was used so that a scalar potential does not appear in the equation for $\vec{B}$. Also, $\vec{\nabla} \cdot \vec{A} = 0$ is then enforced. This is also directly analogous to the incompressibility condition, $\nabla \cdot \vec{q} = 0$, which is continuing on this formulation for the surface reflection conditions. We are currently investigating the properties of this formulation under reflection.

A simpler scalar formulation where the pulse is concentrated near a discontinuity of the scalar, as in the acoustic equation, is also described in Sec. 4.

4. NUMERICAL RESULTS

4.1 Level Set Formulation

We have applied our method to the cases of 2 and 3 dimensions with reflection and refraction, also including curved boundaries. Figure 1 shows an expanding circle in a medium of index of refraction 1 in such a setting using our algorithm. As time increases, more and more reflections take place, leading to wavefronts that almost fill up spatial space. Note our approach not only handles the multiple reflections, which lead to complicated multivalued solutions, but resolves well the wavefronts which have grown in length. Figure 2 shows the cases of reflecting to the curved boundaries. For the cases with both reflection and refraction, in figure 3 and 4, we set the two materials with different index of reflection. As time goes on, as soon as our expanding circle hits the other material, both reflection and refraction take place simultaneously. Finally, Figure 5, 6 and 7 show the three dimensional cases with different initial settings (sphere, ellipsoid, torus).

4.2. Lattice Confinement Formulation

In all of the cases, Lattice Confinement was added to the linear wave equation with simple, second order central discretization.

4.1 Reflection from Planar Surface

In the first demonstration, a uniform Cartesian grid was used with reflection on the walls of a square region, in 2-D as well as 3-D. In general, it is well known that a "tail" will develop behind a 2-D wave front, while the front remains sharp (if it is initially sharp). In the 2-D computation with Confinement we can keep a sharp pulse and suppress the tail. This tail is smooth and could, if desired, be computed using standard CFD on the grid. The goal, however, is to show that a pulse can propagate over long distances with Lattice Confinement. The same long distance propagation was observed in 3-D where there were genuine pulse solutions.

In Fig.9 2-D results are presented for a 128x128 cell grid. It can be seen that there is no perceptible diffusion of the pulse, even after many reflections. These results were also presented in [FWS].

4.2 Scattering from Missile

This computation involved multiple body-fitted grids used. The first missile computation involved a planar scalar wave impinging on the nose of a missile. The plane of the wave is parallel to the longitudinal axis of the missile. The magnitude of the scalar is presented in planes parallel (i.e., the symmetry plane) and perpendicular to the longitudinal axis of the missile, and on the surface of the missile body. Figures 10 and 11 depict the intensity of the planar wave before, during, and after reflection from the missile surface in the nose area from the side and from the front, respectively.

The second computation involved the aft-end of the missile. Figure 12 depicts the same sequence, but in the fin area, as seen from the rear. The third computation involved the entire missile. Figure 13 depicts a pulse reflecting from the nose area at 45°, in the symmetry plane, as seen from the side.

Figure 14 depicts part of the overlapping computational grid. The confinement method has been generalized to curvilinear grids for this case. Besides keeping the pulse sharp, Confinement also prevents reflections from the grid interface regions and thus represents an important capability.

All of the missile results involve a pulse confined to about 3 grid cells except in the fine grid region very near the surface. There, the method reverts to standard CFD. Also, it can be seen in Fig.12 that, unlike in geometrical optics, there is a diffracted component. This will most likely represent a diffracting pulse corresponding to the width of the computational one. We should be able to make corrections to the diffracted intensity to simulate pulses of other widths. This would result in a very general method able to treat diffraction to first order (in this short pulse limit). We are currently studying this possibility.

4.3 Scattering from Aircraft

Next, results of confinement are presented for scattering from an aircraft shape. Here, a uniform Cartesian grid was used with a treatment of the surface boundary conditions involving interpolation. A level set description of the body was used, which was early derived from a surface definition "STL" file. This is shown in Fig. 15. With these boundary conditions, it can be seen that scattering from very complex shapes can easily be computed since body fitted grids are not required. In Fig. 16, contours of the scalar magnitude representing the electromagnetic field in a cross plane near the back of the wing are shown for three different times.

The next results involve the new vector potential computation. There, a single contour can be used to represent each part of the wave since the potential extends throughout the field and has a definite range of values within the pulse. Preliminary results are depicted in Fig. 17 for two times. Further work is progressing on the new technique.

The last results depict a scalar version of the vector potential method showing scattering in the cross plane depicted in Fig. 15. A contour representing the centroid of the pulse is shown in Fig. 18, as a dashed line. Other contours showing the range of values of the scalar are also shown.

REFERENCES

[BK] O. Bruno, and L. Kunyansky, "A Fast, High-Order Algorithm for the Solution of Surface Scattering Problems: Basic Implementation, Tests, and Applications", Journal of Computational Physics 169, 80-110, 2001.

[CKOST] L.-T. Cheng, M. Kang, S. Osher, H. Shim, Y.-H. Tsai, "Reflection in a level set framework for geometric optics", Comput. Modeling in Engineering and Sciences, to appear, (2002)

[CLO] L.T. Cheng, H. Liu, and S. Osher, "High-Frequency Wave Propagation in Schrodinger Equation Using the Level Set Method", submitted to JCP

[COQ] L.-T. Cheng, S. Osher, J. Qian, "Level set based Eulerian methods for multivalued traveltimes in both isotropic and anisotropic media", Society of Exploration Geophysics, submitted

[CSE] J. Caruthers, J. Steinhoff, R. Engels, "An Optimal Finite Difference Representation for a Class of Linear PDE's with Application to The Helmholtz Equation" , *Journal of Computational Acoustic*, Vol.7, No.4, 1999, pp.245-252.

[FEO] E. Fetemi, B. Engquist, and S. Osher, "Numerical Solution of the High Frequency Asymptotic Expansion for the Scalar Wave Equation", Journal of Computational Physics 120, 1995.

[FWS] M. Fan, L. Wang, and J. Steinhoff, "Computation of Short Wave Equation Pulses Using Nonlinear Solitary Waves", to be published in *Computer Modeling in Engineering & Sciences*.

[H] A. Harten, "The Artificial Compression Method for Computation of Shocks and Contact Discontinuities III, Self-Adjusting Hybrid Schemes," *Mathematics of Computation*, Vol. 32, No. 142, 1978.

[JO] Shi Jin, and S. Osher, "A Level Set Method for the Computation of Multivalued Solutions to Quasi-Linear Hyperbolic PDEs and Hamilton-Jacobi Equations", submitted to Comm. Math. Sci.

[L] P.D. Lax, "Hyperbolic Systems of Conservation Laws II", Comm. Pure Appl. Math 10, 1957.

[M] C. Min, "Simplical Isosurfacing in Arbitary Dimension and Codimension.", UCLA CAM Report 03-07(2003), will appear on J. Comput Phys.

[MO] C. Min, and S. Osher, "Local Level Set Method in Arbitrary Dimension and Codimension", in preparation.

[OCKST] S. Osher, L.-T. Cheng, M. Kang, H. Shim, and Y-H Tsai, "Geometric optics in a phase-space-based level set and Eulerian framework", J. Comput Phys., v179, p622-648 (2002)

[QCO] J. Qian, L.-T. Cheng, and S. Osher, "A level set based Eulerian approach for anisotropic wave propagation", submitted to Wave Motion

[S] V. Shankar, "Progress in the Development and Application of Time-Domain CEM", AFOSR Electromagnetics Workshop, Jan. 11-13, 2001.

[SDHXLF] J. Steinhoff, W. Dietz, S. Haas, M. Xiao, N. Lynn, M. Fan, "Simulating Small Scale Features in Fluid Dynamics and Acoustics as Nonlinear Solitary Waves", *AIAA Conference,* Reno, Nevada, Jan. 6-9, 2003

[SU] J. Steinhoff, and D. Underhill, "Modification of the Euler Equations for Vorticity Confinement Application to the Computation of Interacting Vortex Rings," *Physics of Fluids*, 6, 1994.

[SWUP] J. Steinhoff, Y. Wenren, D. Underhill, and E. Puskas, "Computation of Short Acoustic Pulses," Proceedings 6th International Symposium on CFD, Lake Tahoe, Sept., 1995.

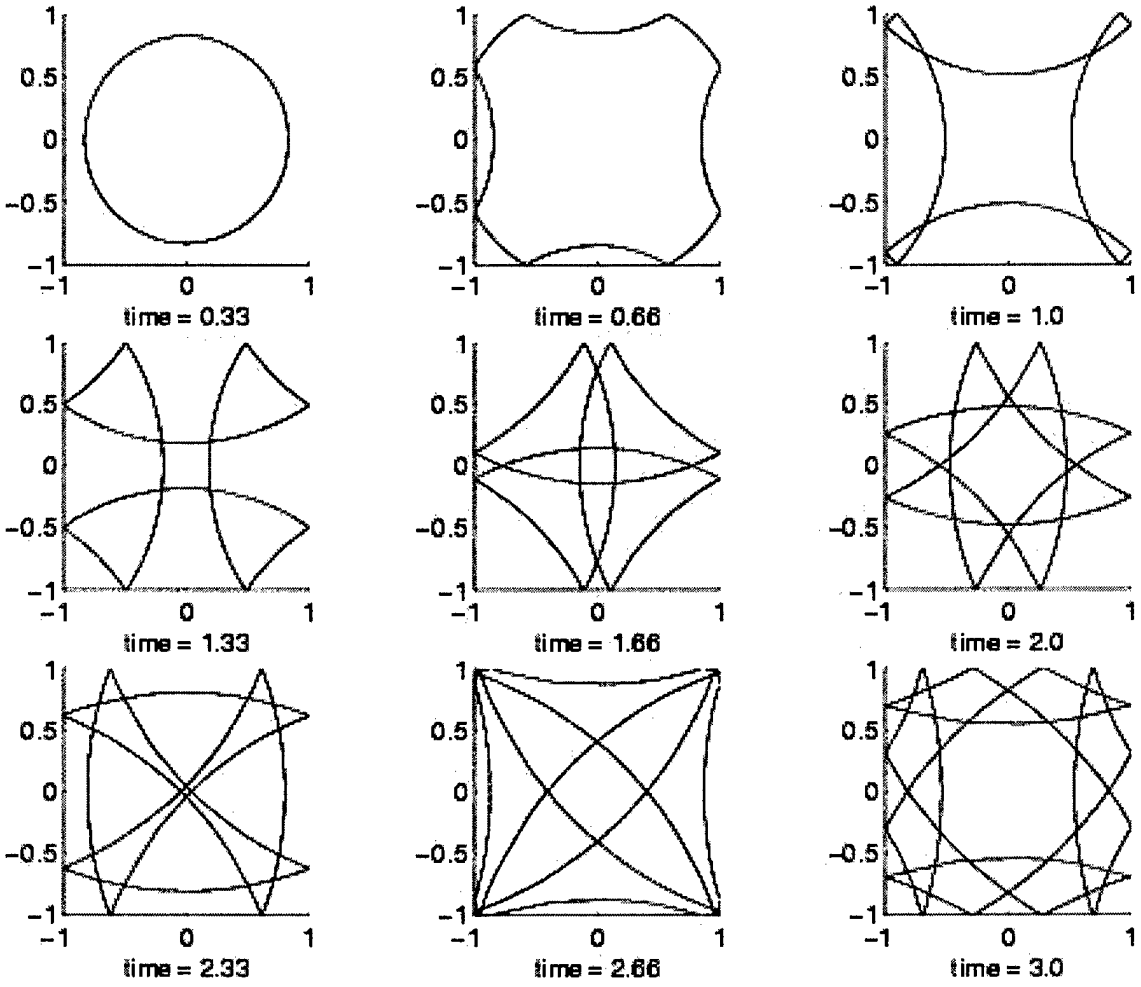

Figure 1

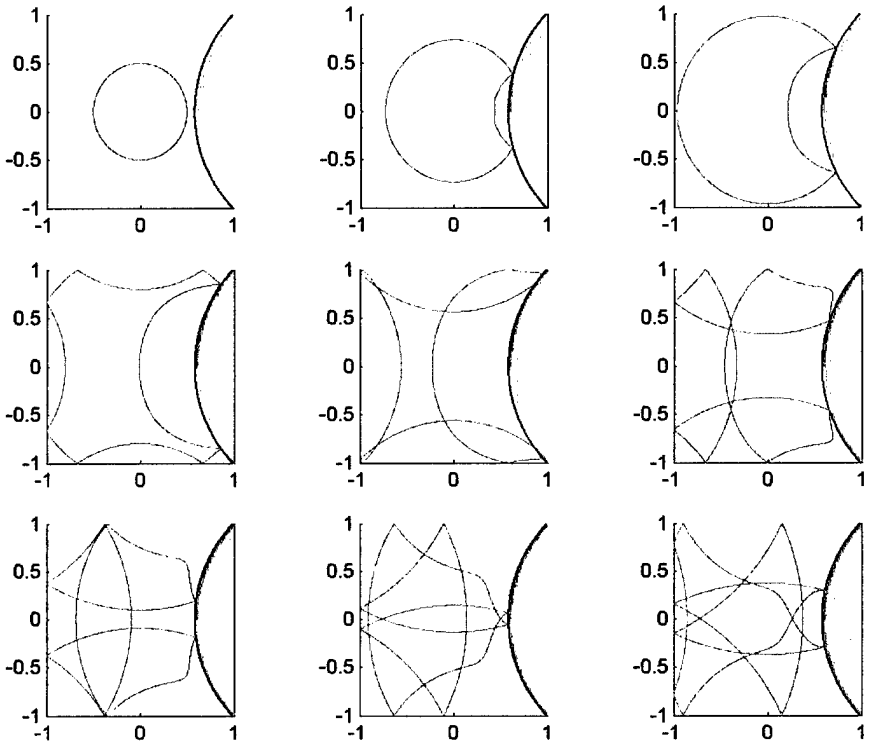

Figure 2

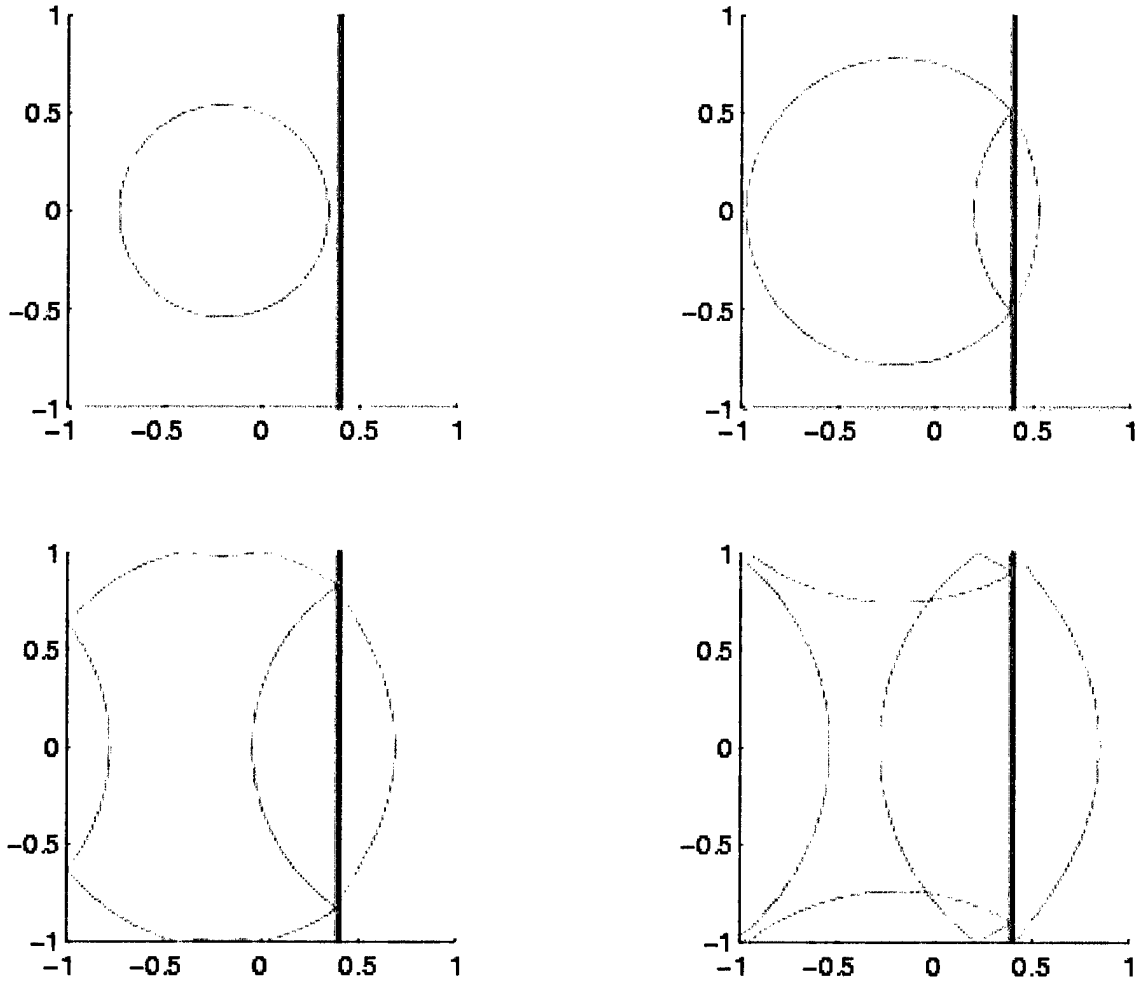

Figure 3

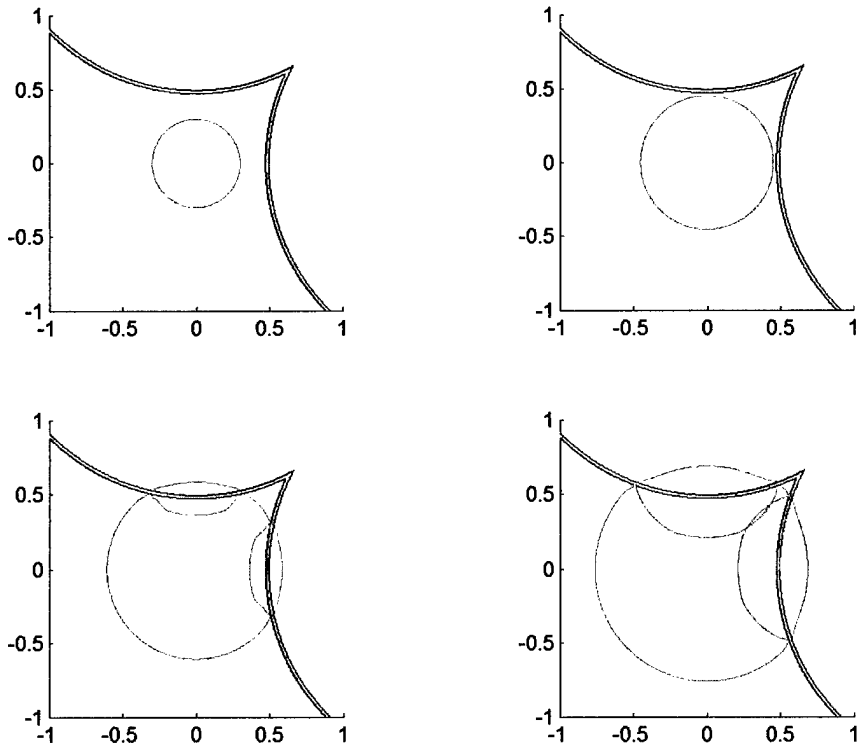

Figure 4

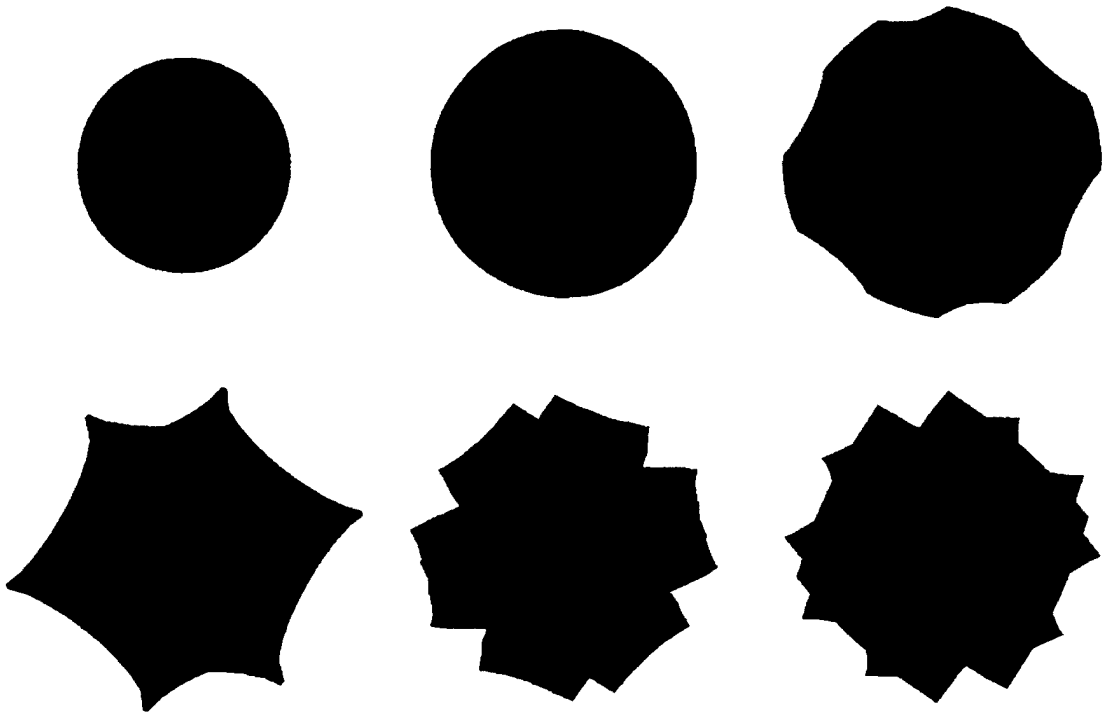

Figure 5

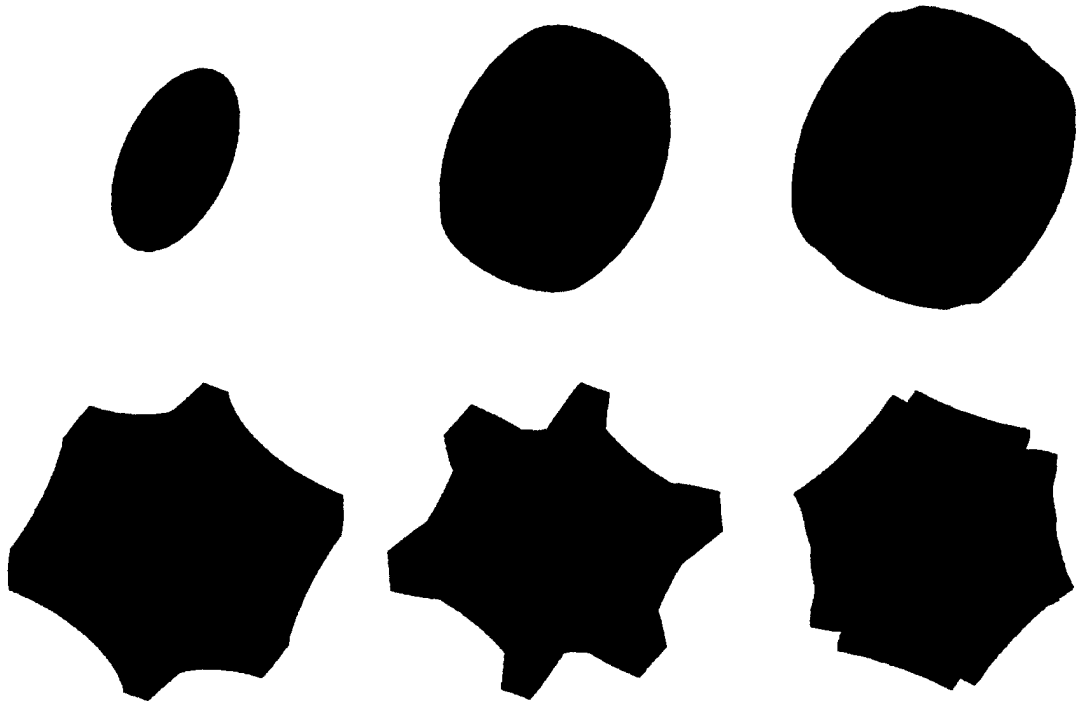

Figure 6

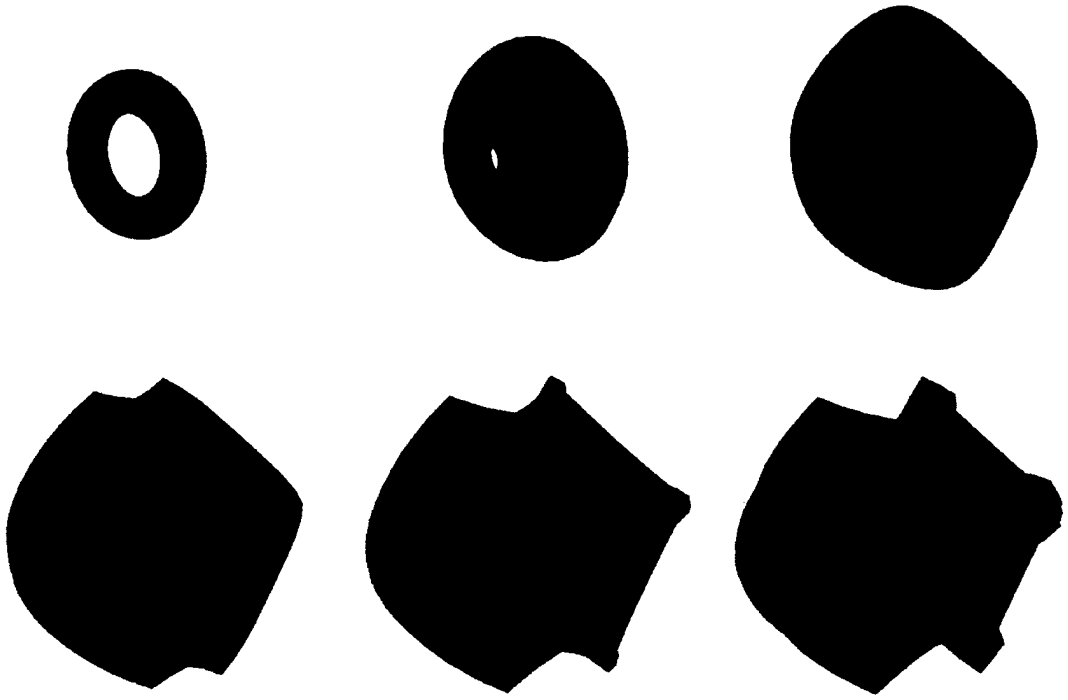

Figure 7

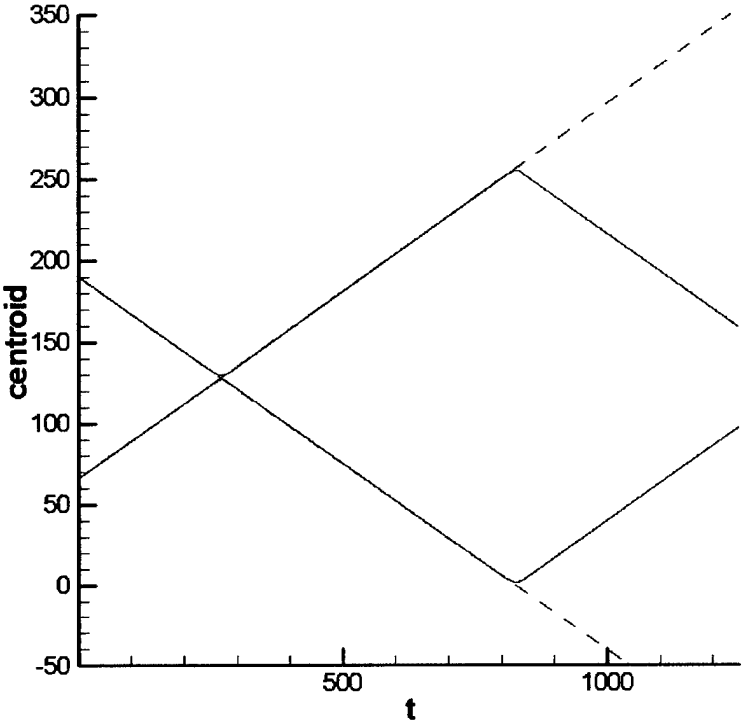

Figure 8. Comparison of Computed Centroid of Pulses with Exact Solution

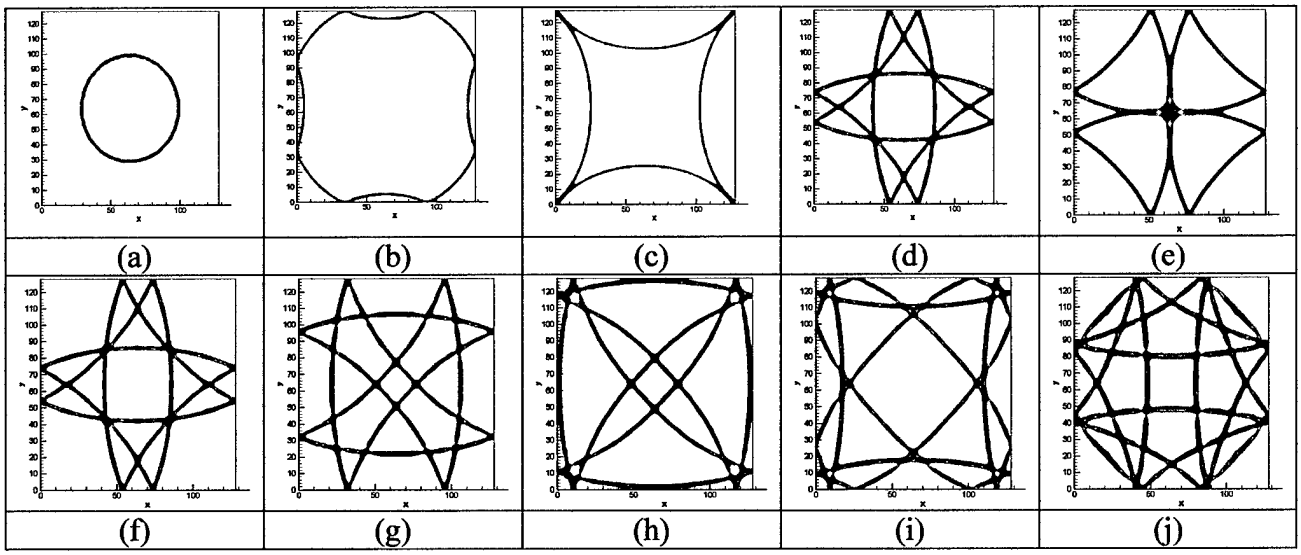

Figure 9.a~j 2D convex wave propagation

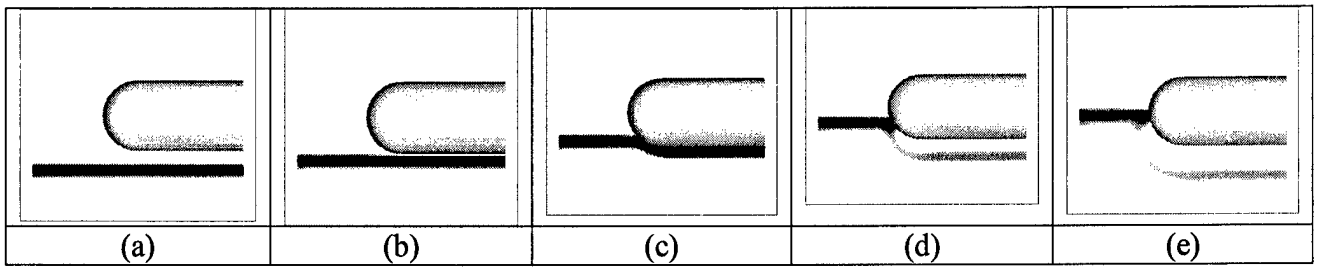

Figure 10.a~e Pulse reflection from missile nose

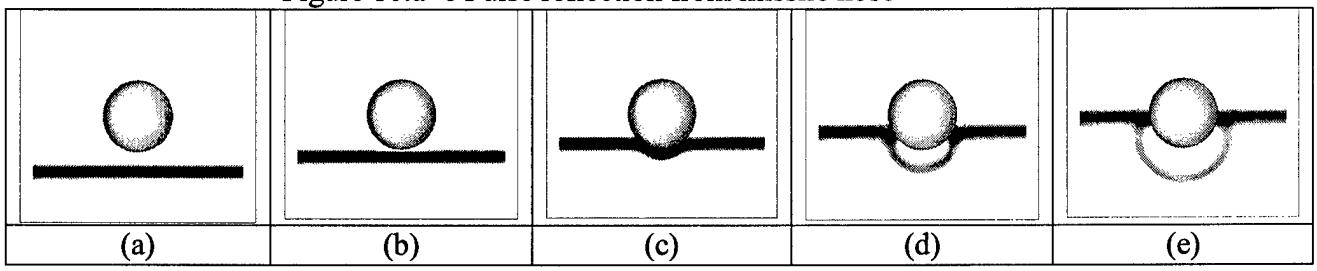

Figure 11.a~e Pulse reflection from missile nose

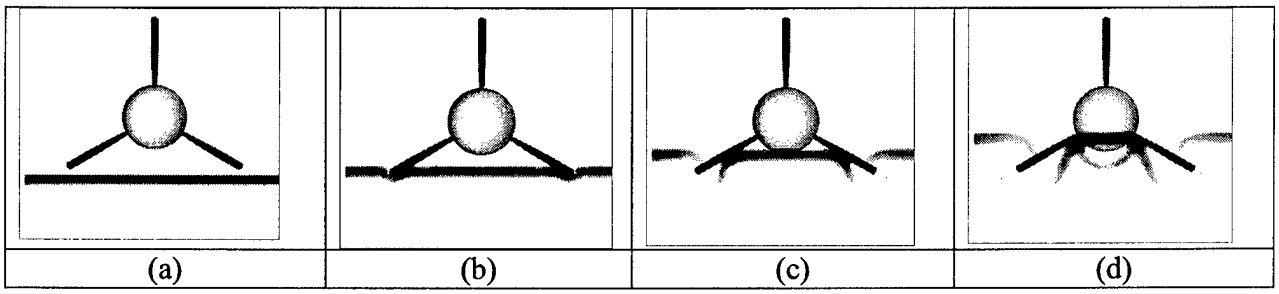

Figure 12.a~d Pulse reflection from missile fins

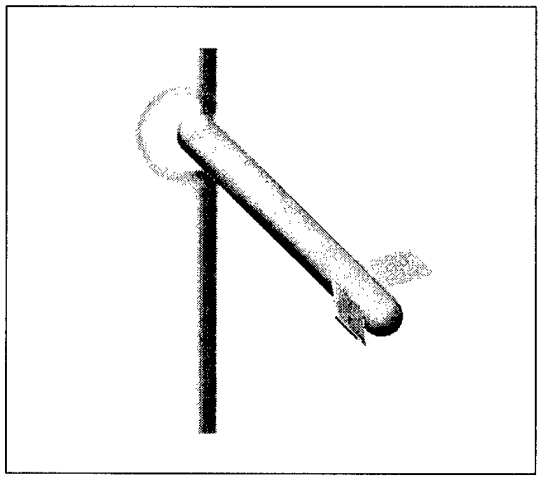

Figure 13. Pulse reflection from missile

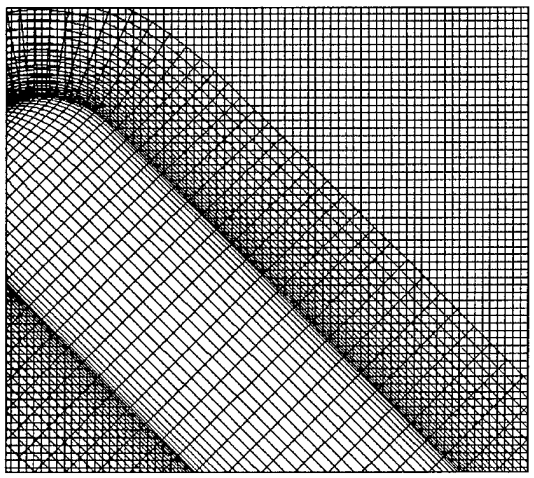

Figure 14. Detail of Missile Grid/ Cartesian Grid Overlap Region

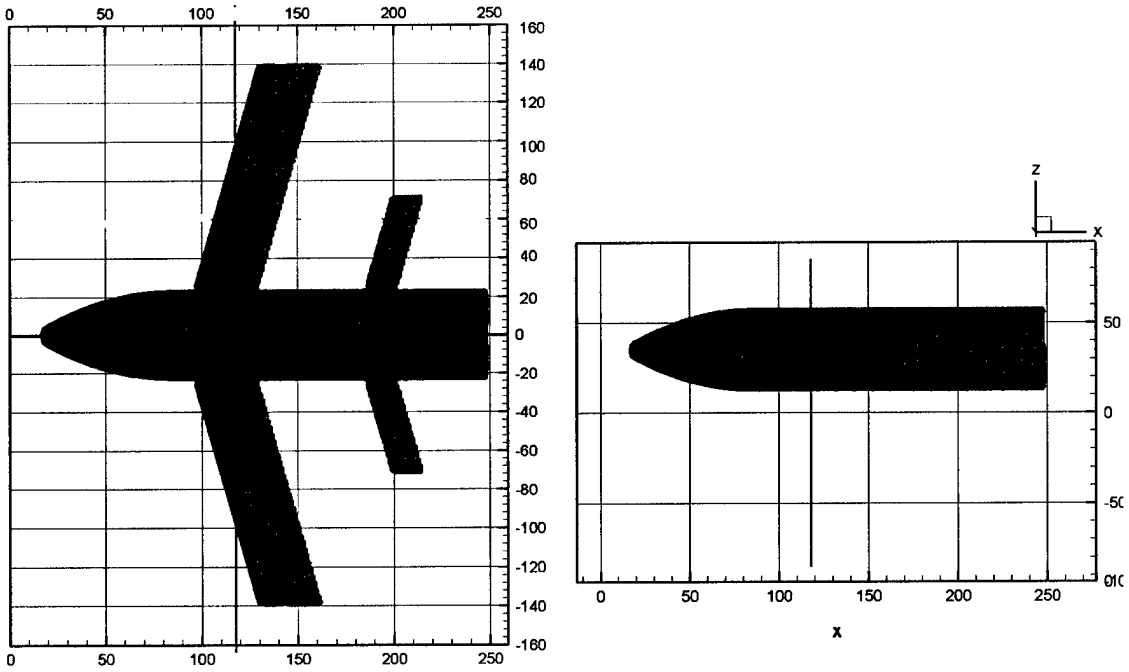

(a) (b)

Figure 15.a~b Aircraft Configuration

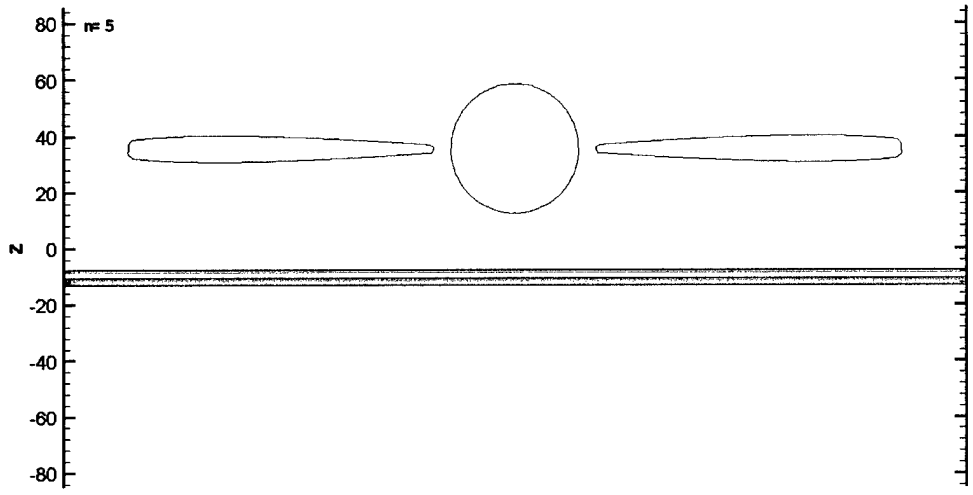

(a)

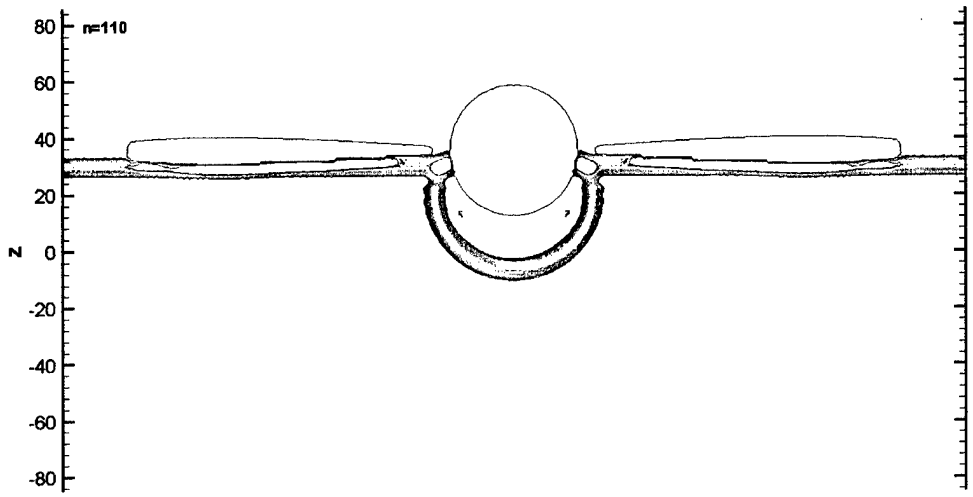

(b)

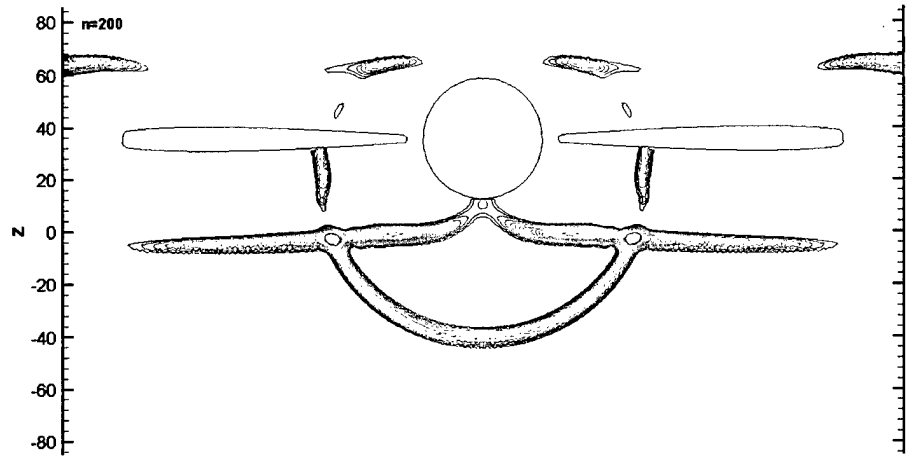

(c)

Figure 16.a~c Contour levels (from one third of the maximum to maximum level) of the scalar with vorticity confinement at different time steps

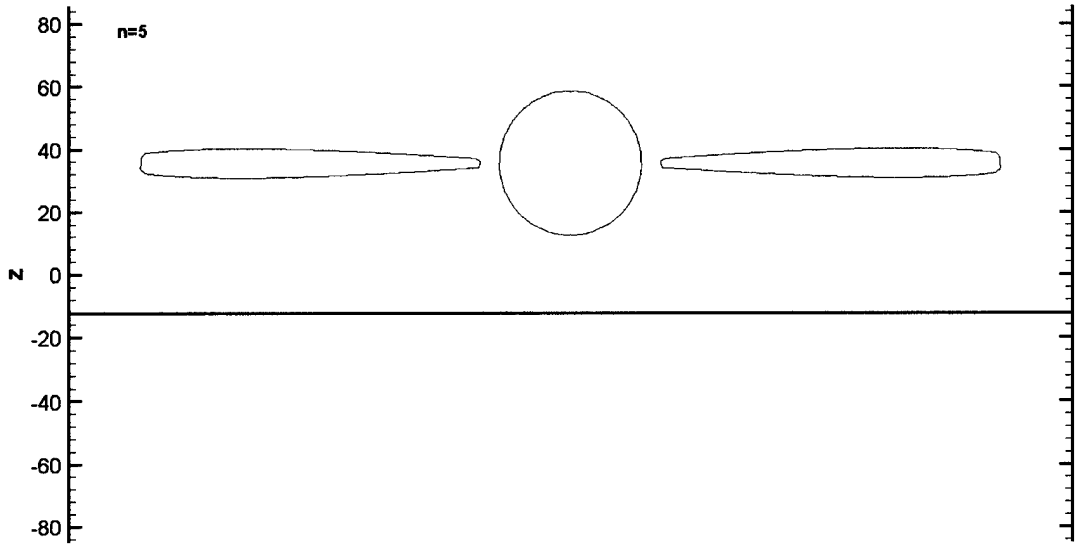

(a)

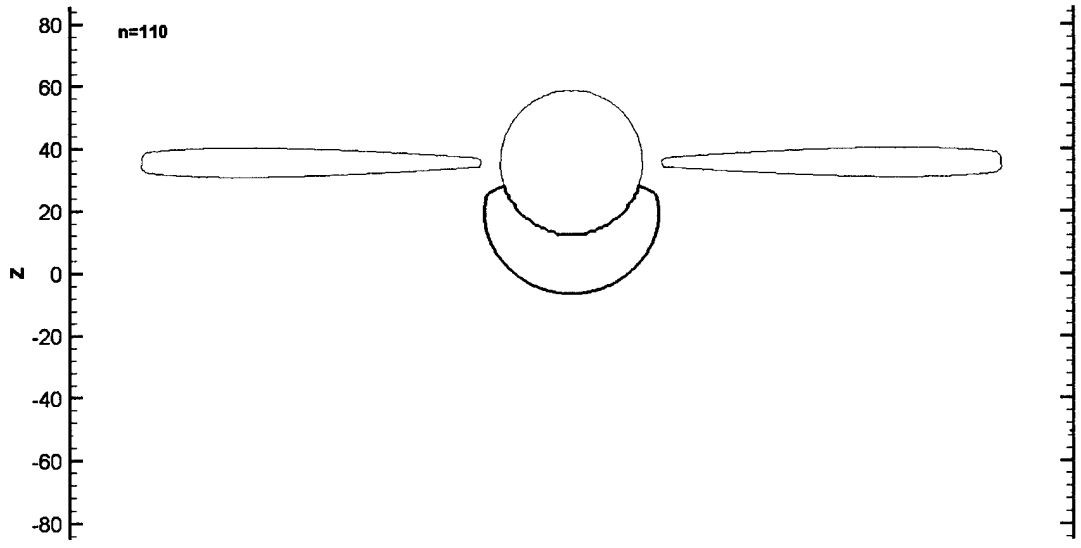

(b)

Figure 17.a~b Contour line (maximum level) of the vector potential magnitude at different time steps

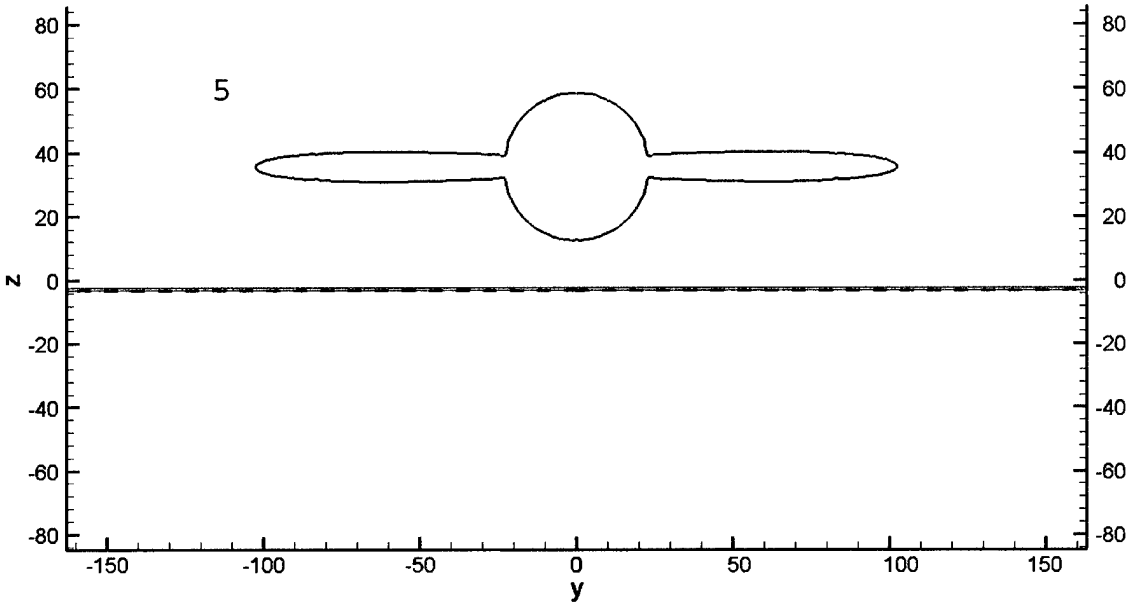
5
80
60
40
20
0
-20
-40
-60
-80
z
-150
-100
-50
0
50
100
150
y

(a)

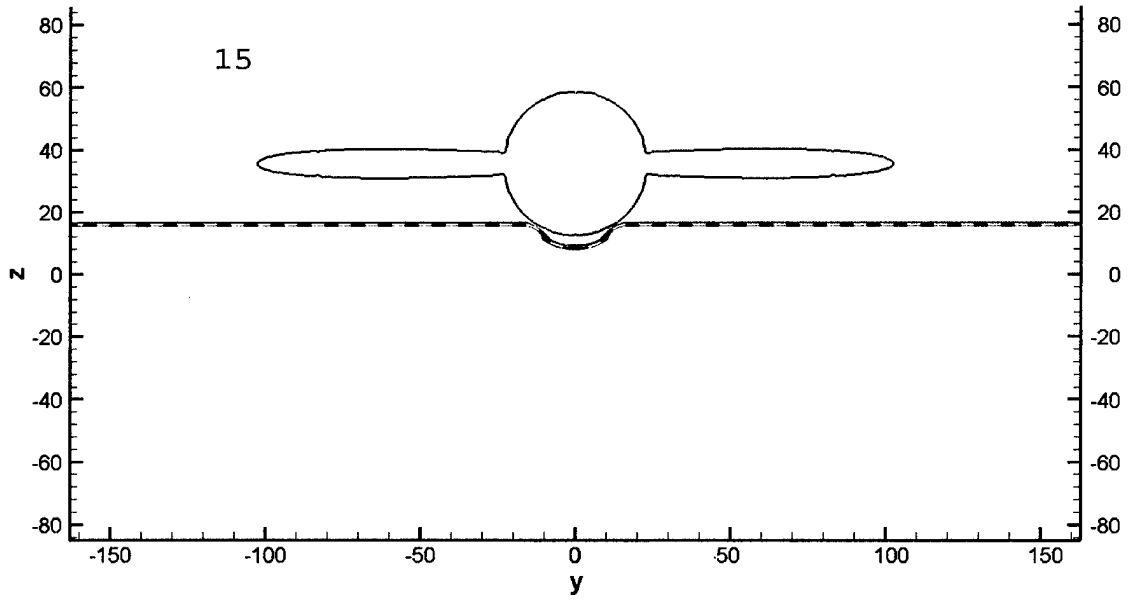
15
80
60
40
20
0
-20
-40
-60
-80
z
-150
-100
-50
0
50
100
150
y

(b)

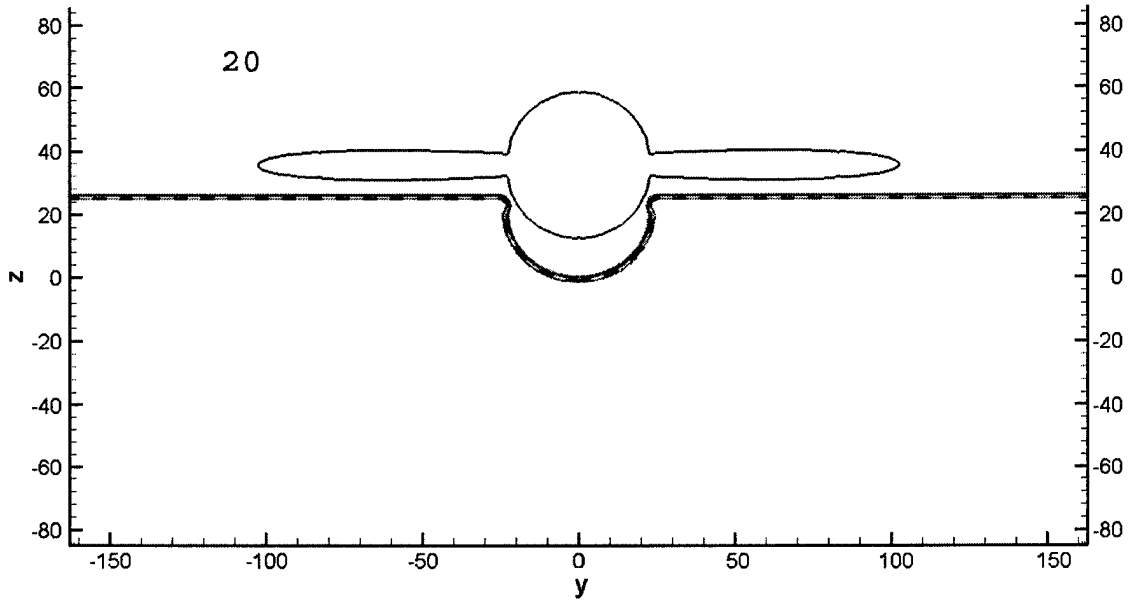
20
80
60
40
20
0
-20
-40
-60
-80
z
-150
-100
-50
0
50
100
150
y

(c)

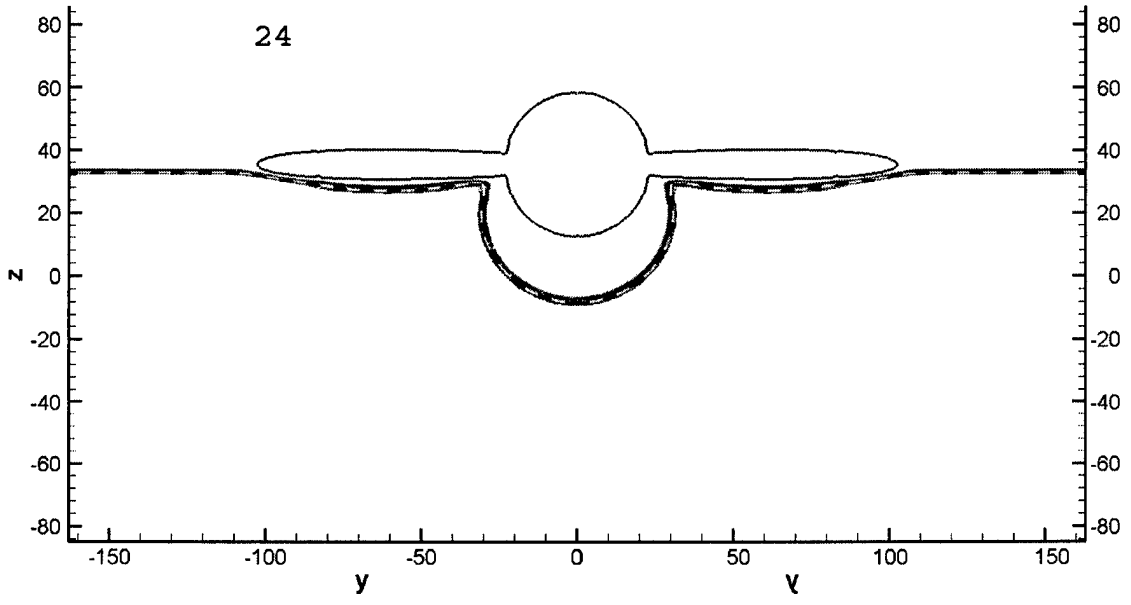
24
80
60
40
20
0
-20
-40
-60
-80
z
-150
-100
-50
0
50
100
150
y

(d)

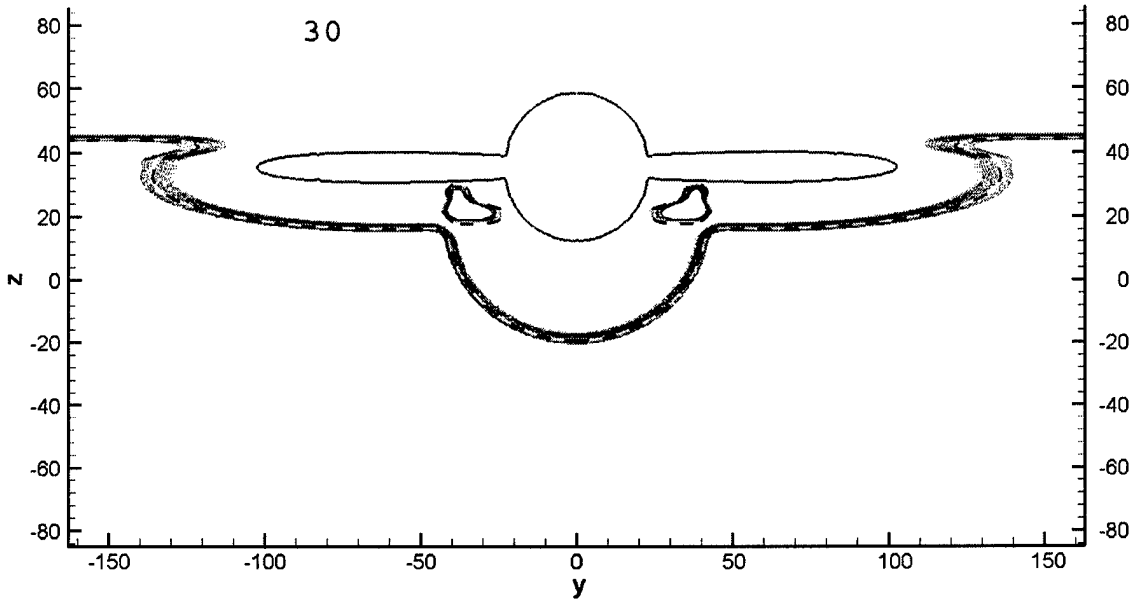

(e)

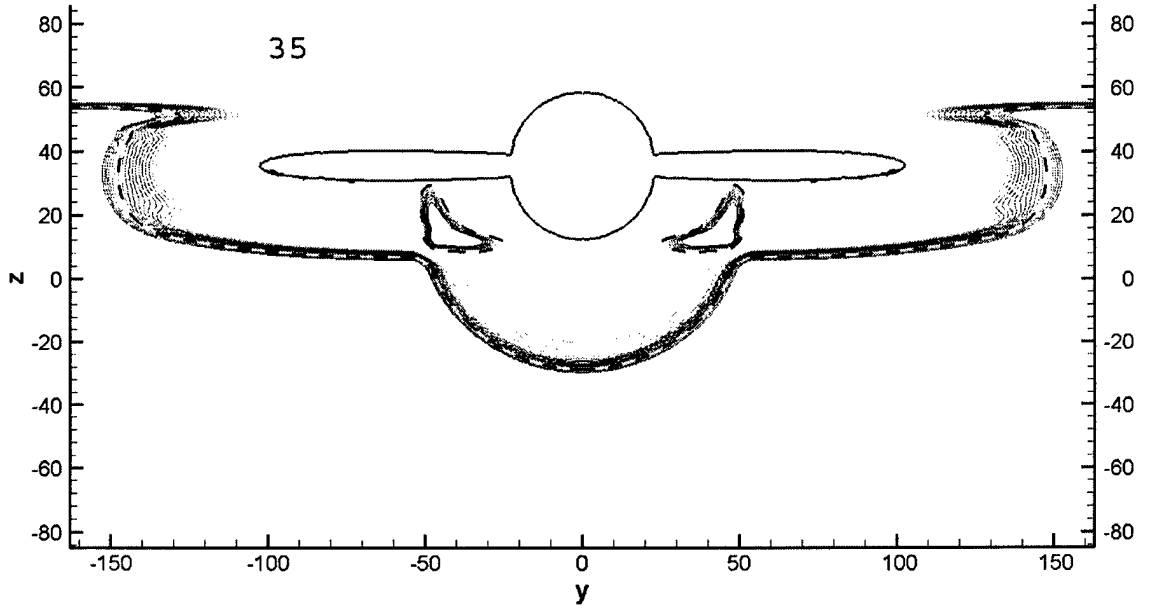

(f)

Figure 18.a~f Scattered scalar wave